A Strategy for Scleroglucan Production in *Sclerotium Rolfsii*: Lowering pH in Fermentation Process by Manipulating Oxalate Metabolic Pathway With CRISPR/Cas9 Tool

Tianlong Bai
Shenyang University of Chemical Technology
Teng Wang
Huazhong University of Science and Technology
Yan Li
Shenyang University of Chemical Technology
Na L Gao
Huazhong University of Science and Technology
Lixin Zhang
Shenyang University of Chemical Technology
Wei-Hua Chen
Huazhong University of Science and Technology
Xiushan Yin (xiushanyin@gmail.com)
Shenyang University of Chemical Technology https://orcid.org/0000-0001-8124-7387

Research

Keywords: AAT1, CRISPR/Cas9, oxalate, scleroglucan, Sclerotium rolfsii

Posted Date: September 22nd, 2020

DOI: https://doi.org/10.21203/rs.3.rs-68434/v1

Version of Record: A version of this preprint was published at Fungal Biology and Biotechnology on February 18th, 2021. See the published version at https://doi.org/10.1186/s40694-021-00108-5.

Abstract

Background: *Sclerotium rolfsii* is a potent producer of many secondary metabolites, one of which like scleroglucan is an exopolysaccharide (EPS) appreciated as a multipurpose compound applicable in many industrial fields.

Results: We chose AAT1 gene in oxalate metabolic pathway as target of CRISPR/Cas9. When the AAT1 gene is disrupted, oxalate was not converted to α-ketoglutarate (AKG), but accumulated. So AAT1-mutant serves to lower the pH (pH 3-4) to increase the production of the pH-sensitive metabolite scleroglucan to be 21.03 g l^{-1} with productivity reached 0.25 g/(L·h).

Conclusions: We established a platform for gene editing to rapidly generate and select mutants, and provide a new beneficial strain of *S. rolfsii* as a scleroglucan hyper-producer which could also reduce the cost of controlling optimum pH condition in fermentation industry.

Background

Microbial biopolymers have been discovered as novel materials to replace plant gums 30 years ago [1]. The advantages of microbial polysaccharides are sustainable production and high quality [2]. In addition, EPS from microorganism is often easy to recover [3]. So it has attracted widespread attention in recent years. For example, pullulan from *Aureobasidium pullulans*, xanthan from *Xanthomonas sp.*, hyaluronic acid from *Streptococcus zooepidemicus*, scleroglucan from *Sclerotium rolfsii* (Teleomorph: *Athelia rolfsii*) have been reported [4–6]. Because of unique structure and high molecular weight, scleroglucan has many properties so that it could be applied in oil recovery [7], food industry [8] and the pharmaceutical industry [9]. Scleroglucan is produced mainly via microbial fermentation. Meanwhile, it has many limits such as low yield and high production cost, which severely hinder scleroglucan application in a wider range of industries [10].

Other factors such as phosphate levels or initial pH do influence scleroglucan production in a much lesser extent [7]. Many researchers have attempted to select the type and concentration of carbon source to affect the production of scleroglucan. The mechanism of scleroglucan production is not clear. Although, some studies have also demonstrated that pH plays a significant role in the fermentation process [11], there is no research of increasing the production of scleroglucan by manipulating relative metabolic pathways at the genomic level.

Oxalic acid is the main acidic metabolite in *S. rolfsi*, and in many other fungi such as *Sclerotinia sclerotiorum* [12]. Oxalic acid is also reported to be directly toxic to plant tissue [13], for it is a strong acid among organic acids and is 10,000 times more acidic than acetic acid. So it could also influence the pH in the process of liquid fermentation to produce scleroglucan. And we also performed bioassays of fungus mutants for indicating more oxalic acid could be produced. For generating a new strain of *S. rolfsii* that is more suitable for fermentation industrial, an appropriate adjustment of oxalate biosynthesis pathway at the genetic level to further increase the production of scleroglucan is in high demand.

The clustered regularly interspaced short palindromic repeats (CRISPR) and CRISPR-associated (CRISPR-Cas9) system has rapidly progressed as an efficient genome editing technique in various organisms, including many ascomycetes and several basidiomycete fungi [14]. Currently, there is limited information about manipulating *S. rolfsii* at genetic level, owing to technical limitations including lack of well-annotated genome and efficient recombinant DNA methodologies. Few reports described the transgenic strains based on protoplast transformation [15–16]. However, there is no gene disruption linked with precise phenotype analysis reported. Recently the draft of *S. rolfsii* genome was published [17]. By combining the transcriptome data [18] and cross-species sequence homology analysis, we were able to obtain the transcripts for essential enzymes for oxalate synthesis, which offered a roadmap for establishing mutant strains that is of indirect relevance for production of scleroglucan with high yields.

Results

Identification of transformation for pDHt/sk-PE plasmid by PCR and fluorescence microscopy

To test whether transgene line could be established in *S. rolfsii*, we performed the pDHt/sk-PE plasmid transformation with the PEG based method. After 5 days in hygromycin-PDA medium, the eGFP signal can be consistently detected. The PCR analysis with eGFP primers showed the positive band (Figure 1A). Then, we observed the bright fluorescent signal in hypha of transformants by fluorescence microscopy (Figure 1B), indicating the transformed strains contain the functional elements. Altogether, we have established the convenient method for PEG-based pDHt/sk-PE transformation.

CRISPR/Cas9 mediated gene inactivation in *S. rolfsii*

To transfer Cas9 RNPs (ribonucleoprotein complex) targeting AAT1, we used the PEG-mediated transformation method to deliver RNP into fungal protoplasts, with selecting plasmid Htb2-GFP which carrying the hygro cassette. And we also co-transformed Cas9 expressing plasmid pDHt/sk-PE and guide RNA complex to knock out AAT1 simultaneously. AAT1-MT colonies were confirmed by sequencing (Figure 2A). In fact, they could be quickly selected by the yellow color they caused in hygromycin-BPDA medium among hundreds of colonies (Figure 2B). Because the early appearance of yellow color is due to that AAT1-MT colonies have produced more acid metabolites than WT. HPLC-MS was used to identify which acid they secreted here played a major role.

Disruption AAT1 leads to elevated both oxalic acid and scleroglucan production

Metabolic pathway of AAT1-MT is showed in Figure 3A. Based on the measurement of the oxalic acid peak area (Figure 3B), we calculate that the concentrations of oxalic acid in WT and AAT1-MT samples are 843.32 μg ml-1 and 2854.42 μg ml-1, respectively. And we also analyzed AKG, the close related metabolite in this pathway (supplementary figure s3). The mass spectrograms are showed in supplementary figure s4. Above all, the mutant strains secreted 3 times more of oxalate than WT and significantly less of AKG, indicating the disruption of AAT1 leads to the metabolic flow towards the oxaloacetate direction then produce more oxalic acid. Clearly, due to the inactivation of AAT1 and the

accumulation of oxalic acid, the lesion area in mutant strains was more significant compared to control strains, which is shown with brown color in the leaflets (Figure 3C).

The line chart (Figure 3D) about concentrations of oxalic acid and scleroglucan in fermentation broth showed that the ability of AAT1-MT for producing scleroglucan (21.03 g l-1) is stronger than WT (12.11 g l-1). The scleroglucan production of AAT1-MT is increased by 73.66%, when compared with WT. Dry cell weight (DCW) concentration and pH in the fermentation process was showed in Figure 3E. After 48h, the pH could keep at about 3.37 and the growth of oxalate accumulation slowed. This slow-down coincided with a drop in culture pH to less than 3.5 [19]. This phenomenon could possibly be due to the pre-activation of some degradative enzymes, such as oxalate decarboxylase and oxalate oxidase [18], by a mass of oxalic acid. In other fungi such as *Coriolus versicofor* and *Collybia velutipes*, the optimum pH of these enzymes has been reported to be 3 [20-21]. The highest DCW (14.26g l-1) of AAT1-MT was achieved when pH was at 4 after 36 h, while the DCW of the WT is 10.23 g-1. When pH is between 3 and 4, both cell growth and polysaccharide synthesis is fast-growing. And the scleroglucan productivity reached 0.25 g/(L•h) which increased by 78.57% when compared with that obtained from WT (0.14g/(L•h)).

Discussion

Scleroglucan is a polysaccharide composed of a linear chain of β-(1,3)-linked D-glucopyranosyl residues with single β-(1,6)-linked D-glucopyranosyl groups attached to about every third residue of the main chain [22]. Many excellent properties, including water solubility, pseudoplasticity, moisture retention, salt tolerance, and viscosity stability, deserve us thinking about how to solve its application problem fundamentally.

This is the first study of exploring CRISPR-Cas9 system in *S. rolfsii*. In the CRISPR/Cas9 system, the Cas9 endonuclease catalyzes a DNA double-strand break (DSB) aided by a single-guide RNA (sgRNA) containing a 20-nt sequence that matches the sequence upstream of the protospacer-adjacent motif (PAM; 5’-NGG-3’) site on the target locus. The DSB can then be followed by deletion, insertion, or substitution of the sequence using homology recombination or non-homologous end joining (NHEJ) pathway. Therefore, we aimed at establishing the CRISPR/Cas9 system to change metabolic pathway then more oxalic acid could be produced to change the pH of fermentation liquid that is in favour of scleroglucan production.

We also tried with sgRNA transformation together with Cas9 plasmid. However we only got one mutant colony. Using the Cas9 protein/sgRNA ribonucleoproteins (RNPs) to perform genome editing has several advantages compared with co-transforming of Cas9 expression plasmid and sgRNA. A major advantage is transformation of Cas9 RNPs alleviates the possibility of integration of genetic material to a non-targeted region of the genome [23–24]. Additionally, Cas9 and sgRNA are able to form a stable ribonucleoprotein in vitro, so there is less likelihood of RNA degradation compared with Cas9 mRNA/sgRNA transformation.

Conclusions

So far, most studies mainly cover the feasibility of establishing the CRISPR/Cas9 system in filamentous fungi, only few works have explored the application of genome editing for fungal metabolic engineering [25]. The results of this study provided an effective strategy to indirectly control pH condition, thereby increasing the yield of sclerogulcan by using newly emerging gene editing tool CRISPR/ Cas9, and showed a potential strategy to radically decrease the cost of artificial regulating pH in industrial sclerogulcan fermentation process.

Methods

Strain and culture condition

Sclerotium rolfsii (Teleomorph: *Athelia rolfsii*) deposited in the Chinese Academy of Agricultural Sciences (CAAS), was used as the wild-type (WT) and cultured in potato dextrose agar (PDA; peeled potato 200 g, dextrose 20 g, agar 15 g, distilled water 1 l, pH=7.5) and in the fermentation medium (glucose 130 g, $NaNO_3$ 3 g, yeast extract 1 g, KCl 0.5 g, KH_2PO_4 1 g, $MgSO_4{\cdot}7H_2O$ 0.5 g, distilled water 1 l, pH=7.5) at 30°C. Batch fermentations were performed in a 5-L fermentor containing 3L of fermentation medium. All the components were autoclaved for 20 min at 115°C. The strain was identified by ITS primers. All primers used in this study are listed in supplementary table s1.

AAT1 identification

To identify the AAT1 gene, we first downloaded the assembled genome of *Athelia rolfsii* (GCA_000961905.2) from NCBI and annotated its protein-coding genes using GeneMark-ES [26] with opinions '–ES –fungus –sequence'. We also assembled a transcriptome data available from the NCBI SRA database for *A. rolfsii* (accession ID: SRS025455) using SPAdes [27] with opinions '–sc -s –careful -k 75', and also annotated the protein-coding genes. All the protein-coding genes were combined and renamed starting with A0000000.

We manually selected AAT1 genes from six well-annotated fungal genomes including *Scheffersomyces stipitis, Emiliania huxleyi, Kluyveromyces marxianus, Saccharomyces cerevisiae, Pseudogymnoascus destructans and Candida albicans*) and BLASTed their protein sequences against the identified protein-coding genes of *A.rolfsii* (supplementary figure s1 a). We identified gene "A0001768" from transcriptome data as the best hit. We then confirmed that "A0001768" could cover the full-length of AAT1 by building a multiple sequence alignment using the protein sequences of "A0001768" and the six fungal AAT1 proteins using an online version of Clustal Omega [28-29]. The result was visualized by an online version of Mview [30] later.

Finally, we obtained the gene structure (i.e., the delineation of its exons) of "A0001768" (supplementary figure s1 b) by mapping its coding sequences to its assembled genome using BLAT [31].

Preparation of Cas9 protein, sgRNA and plasmids

Cas9 protein was purchased from New England BioLabs Inc. The protospacer sequences (CAGACCGGGACGACAAACCGTGG) of sgRNA named CR1-AAT1 were designed and screened against targets using Geneious software and confirmed with the online tool CHOPCHOP [32-33]. TrancrRNA and crRNA were purchased from GenePharma (Suzhou China). The assembling of guide RNA complex is described as following: mix 4.5 μl crRNA (50 μM), 4.5 μl trancrRNA (50 μM) and 10 μl duplex buffer well. Incubate the mixture at 95 °C for 5 min and cool down at R.T. for 20 min. All plasmids used in this study and their purposes are listed in supplementary table s2 and they were all purchased from Addgene.

Preparation of protoplast

Procedures of protoplast formation were carried out as described in [34], with some modified details presented here. After 90 min of incubation for depriving the cell wall, we used sterile 100 μm Cell Strainer to filter out impurities of reaction mixture.

Transformation for *S. rolfsii*

PEG-mediated fungal transformation was conducted according to previously described with modifications [35]. Briefly, the RNPs (ribonucleoprotein complexes which are composed of Cas9 and sgRNA) and Htb2-GFP plasmid were prepared during generation of the protoplasts where the Cas9 RNPs were made as follows: 10 μl assembled guide RNA complex (described above) and 5 μl Cas9 protein (50 μM) were added into a 50 μl total volume with 5 μl 10× Cas9 Nuclease Reaction Buffer and DEPC-treated water. This mixture was incubated in a 37°C water bath for 25 min, and 100 μL of fungal protoplasts were mixed with 20 μl Cas9 RNPs and Htb2-GFP plasmid at room temperature for 20 min. Then 40 % PEG was added into the above system and incubated at room temperature for 20 min. After STC buffer (1.2 M Sorbitol, 10 mM pH 7.5 Tris–HCl, 10 mM $CaCl_2$) was mixing well by gently inverting the tubes several times, the total system was directly transferred into MGY regeneration medium (1% malt extract, 1% glucose, 0.1% yeast extract, 2% agar, pH 5.5) with 0.5M sucrose osmotic stabilizer. Four days later, protoplasts developed into incipient colonies observable with the naked eye, then, bottom agar was covered with 20ml top selective hygromycin-BPDA agar containing hygromycin (35 μg ml^{-1}) and bromophenol blue (60 μg ml^{-1}) which is a kind of indicator that changes color from yellow to blue at the pH from 3.0 to 4.6.

Fluorescence microscopy

The subcellular localization of eGFP was carried out using a Leica DMi8 fluorescence microscope. The transformants containing pDHt/sk-PE were cultured in MGY agar plate in the dark incubator at 30°C for 7 days.

Analytical method

Mycelium was obtained by germination of water-preserved sclerotia on PDA agar plate and incubated at 30 °C as previously described [36]. Then, two 250-ml Erlenmeyer flasks of 50 ml of liquid medium (MGY) were inoculated with five mycelium covered agar discs (approx. 5 mm diameter) removed from the 2-day-old PDA culture of WT and AAT1 mutant type (MT), respectively, at 30 °C on an orbital shaker at 250 rev min^{-1} for 45 h waiting for HPLC-MS analysis. Mycelia were frozen in the refrigerator at -80 °C. After thawing, mycelia were grinded in a mortar until mycelium was completely broken and mushy. Equal volume of ethyl acetate was added to extract and collect the ethyl acetate phase under ultrasonic condition (at 100 kHz for 1h). Rotate evaporation was used to dry the phase at 55 ℃, and added 6 ml methanol in a volumetric flask waiting to be tested about metabolites from mycelium itself, like AKG. The HPLC system (Agilent Technologies Inc., California, United States of America) was coupled with MS detector (AB SCIEX, Foster City, CA, USA) equipped with electrospray ionization (ESI) source which has positive and negative modes (ESI+ and ESI−). Reverse phase chromatographic analysis was carried out using a C-18 reverse-phase HPLC column (200 mm×4.6 mm i.d., 5 μm particle size) at 25 °C under isocratic conditions where the concentration of the mobile phase was constant throughout the run. Running conditions included a 10 μl injection volume of mobile phase methanol-0.02% acid ((NH4)2HPO4) (5:95, v/v), flow rate 0.8 ml min^{-1}, and detection at 197 nm. Samples were filtered through a membrane filter (pore size 0.22μm, ANPEL) prior to injection in a sample loop. Standard curve and equation of linear regression were shown in s**upplementary figure s2**. The peak areas of all oxalic acid relative standards and samples are listed in supplementary table s3.

Then we also measured the scleroglucan production in the fermentation broth between WT and AAT1-MT. The fermentation broth was diluted 5 times with distilled water, heated at 70°C for 40min, and then centrifuged at 13400×g for 25min. The precipitate obtained was washed with distilled water and dried at 105°C. An equal volume of absolute ethanol was added to the supernatant to precipitate scleroglucan. The mixture stayed on ice for 12 h to completely precipitate. In the end, the scleroglucan was recovered by vacuum drying [37].

Bioassays of acid metabolites

In order to identify that AAT1-MT could produce more acid metabolites than WT, bioassays were performed using detached peanut leaflets inoculated with an agar plug of *S. rolfsii* mycelia. *S. rolfsii* cultures were grown on potato dextrose agar plates and 5-mm plugs taken from the actively growing edge. Leaflets were wounded with a knife for 5mm on the adaxial surface, near the midvein, and plugs were placed on the open wounds. Five leaflets were inoculated for each plant line tested using a minimal quantity of agar in each plug. The plates were incubated for 36 h at 30 °C, and lesion area shown brown blight color caused by oxalic acid.

Statistical analysis

All the WT and AAT1-MT mycelium samples were designed for three biological replicates. The data from repeated HPLC analyses were pooled and subjected to ANOVA for statistical significance by least

significance difference (LSD) test at P=0.01. An independent sample t-test was used for statistical evaluations between the WT and AAT1-MT groups ($P \leq 0.05$) by the SPSS 21.0 software (IBM, Chicago, IL, USA).

Abbreviations

AKG: α-ketoglutarate; CRISPR: clustered regularly interspaced short palindromic repeats; crRNA: CRISPR-RNA; DCW: dry cell weight; DSB: double-strand break; EPS: exopolysaccharide; gRNA: guide RNA; NHEJ: non-homologous end joining; PAM: protospacer adjacent motif; sgRNA: single guide RNA; RNPs: ribonucleoprotein complexes;

Declarations

Acknowledgements

We acknowledge Professor Yan from the Chinese Academy of Agricultural Sciences for her generous gift of the *S. rolfsii* strain.

Authors' contributions

TB performed the experiment. TW and NLG performed the data analyses. YL and LZ contributed to the HPLC-MS analysis. WC contributed significantly to the data analyses. XY contributed to the conception of the study and manuscript preparation.

Funding

This work was supported by the National Natural Science Foundation of China (No.81472095).

Availability of data and materials

Not applicable.

Ethics approval and consent to participate

Not applicable.

Consent for publication

Not applicable.

Competing interests

The authors declare no conflict of interest.

References

1. Paul F, Morin A, Monsan P. Microbial polysaccharides with actual potential industrial applications. Biotechnol Adv. 1986;4:245-259.
2. Freitas F, Torres CAV, Reis MAM. Engineering aspects of microbial exopolysaccharide production. Bioresour Technol. 2017;245:1674-1683.
3. Donot F, Fontana A, Baccou JC, Schorr-Galindo S. Microbial exopolysaccharides: main examples of synthesis, excretion, genetics and extraction. Carbohydr Polym. 2012;87:951-962.
4. Badle SS, Jayaraman G, Ramachandran KB. Ratio of intracellular precursors concentration and their flux influences hyaluronic acid molecular weight in *Streptococcus zooepidemicus* and recombinant *Lactococcus lactis*. Bioresour Technol. 2014;163:222-227.
5. Brumano LP, Antunes FAF, Souto SG, Dos Santos JC, Venus J, Schneider R, da Silva SS. Biosurfactant production by *Aureobasidium pullulans* in stirred tank bioreactor: new approach to understand the influence of important variables in the process. Bioresour Technol. 2017;243:264-272.
6. Wang Z, Wu J, Zhu L, Zhan X. Activation of glycerol metabolism in *Xanthomonas campestris* by adaptive evolution to produce a high-transparency and low-viscosity xanthan gum from glycerol. Bioresour Technol. 2016;211:390-397.
7. Schmid J, Meyer V, Sieber V. Scleroglucan: biosynthesis, production and application of a versatile hydrocolloid. Appl Microbiol Biotechnol. 2011;91:937-947.
8. Castillo NA, Valdez AL, Farina JI. Microbial production of scleroglucan and downstream processing. Front Microbiol. 2015;6:1106.
9. Coviello T, Palleschi A, Grassi M, Matricardi P, Bocchinfuso G, Alhaique F. Scleroglucan: aversatile polysaccharide for modified drug delivery. Molecules. 2005;10:6-33.
10. Tan R, Lyu Y, Zeng W, Zhou J. Enhancing scleroglucan production by *Sclerotium rolfsii* WSH-G01 through a pH-shift strategy based on kinetic analysis. Bioresour Technol. 2019;293:122098.
11. Schilling BM, Henning A, Rau U. Repression of oxalic acid biosynthesis in the unsterile scleroglucan production process with *Sclerotium rolfsii* ATCC 15205. Bioprocess Eng. 2000;22:51-55.
12. Monazzah M, Rabiei Z, Enferadi ST. The effect of oxalic acid, the pathogenicity factor of *Sclerotinia Sclerotiorum* on the two susceptible and moderately resistant lines of sunflower. Iran J Biotechnol. 2018;16:e1832.
13. Kyoung SK, Min JY, Dickman MB. Oxalic acid is an elicitor of plant programmed cell death during *Sclerotinia Sclerotiorum* disease development. Mol Plant Microbe Interact. 2008;21:605-12.
14. Kunitake E, Tanaka T, Ueda H, Endo A, Yarimizu T, Katoh E, Kitamoto H. CRISPR/Cas9-mediated gene replacement in the basidiomycetous yeast *Pseudozyma antarctica*. Fungal Genet Biol. 2019;130:82-90.
15. Yasokawa D, Shimizu T, Nakagawa R, Ikeda T, Nagashima K. Cloning, sequencing, and heterologous expression of a cellobiohydrolase cDNA from the basidiomycete *Corticium rolfsii*. Biosci Biotechnol Biochem. 2003;67:1319-26.

16. Sharma M, Schmid M, Rothballer M, Hause G, Zuccaro A, Imani J, Kämpfer P, Domann E, Schäfer P, Hartmann A, Kogel KH. Detection and identification of bacteria intimately associated with fungi of the order Sebacinales. Cell Microbiol. 2008;10:2235-46.
17. Iquebal MA, Tomar RS Parakhia MV, Singla D, Jaiswal S, Rathod VM, Padhiyar SM, Kumar N, Rai A, Kumar D. Draft whole genome sequence of groundnut stem rot fungus *Athelia rolfsii* revealing genetic architect of its pathogenicity and virulence. Scientific Reports. 2017;7:5299.
18. Schmid J, Muller-Hagen D, Bekel T, Funk L, Stahl U, Sieber V, Meyer V. Transcriptome sequencing and comparative transcriptome analysis of the scleroglucan producer *Sclerotium rolfsii*. BMC Genomics. 2010;11:329.
19. Culbertson BJ, Krone J, Gatebe E, Furumo NC, Daniel SL. Impact of carbon sources on growth and oxalate synthesis by the phytopathogenic fungus Sclerotinia sclerotiorum. World J Microbiol Biotechnol. 2007;23:1357–1362.
20. Dutton MV, Evans CS, Atkey PT, Wood DA. Oxalate production by Basidiomycetes, including the white-rot species Coriolus versicolor and Phanerochaete chrysosporium. Appl Microbiol Biotechnol. 1993;39:5-10.
21. Kuan IC, Tien M. Stimulation of Mn-peroxidase activity – a possible role for oxalate in lignin biodegradation. PNAS. 1993;90:1242-1246.
22. Farina JI, Sineriz F, Molina OE, Perotti NI. High scleroglucan production by Sclerotium rolfsii: in fluence of medium composition. Biotechnol Lett. 1998;20:825-831.
23. Longmuir S, Akhtar N, MacNeill SA. Unexpected insertion of carrier DNA sequences into the fission yeast genome during CRISPR-Cas9 mediated gene deletion. BMC Res Notes. 2019;12:191.
24. Skryabin BV, Kummerfeld DM, Gubar L. Pervasive head-to-tail insertions of DNA templates mask desired CRISPR-Cas9-mediated genome editing events. Sci Adv. 2020;6:eaax2941.
25. Shi TQ, Liu GN, Ji RY, Shi K, Song P, Ren LJ, Huang H, Ji XJ. CRISPR/Cas9-based genome editing of the filamentous fungi: the state of the art. Appl Microbiol Biotechnol. 2017;101:7435-7443.
26. Ter-Hovhannisyan V, Lomsadze A, Chernoff YO, Borodovsky M. Gene prediction in novel fungal genomes using an ab initio algorithm with unsupervised training. Genome Research. 2008;**18:1979-90.**
27. Bankevich A, Nurk S, Antipov D et al. SPAdes: a new genome assembly algorithm and its applications to single-cell sequencing. J Comput Biol. 2012;19:455-477.
28. Sievers F, Wilm A, Dineen D, Gibson TJ, Karplus K, Li W, Lopez R, McWilliam H, Remmert M, Söding J, Thompson JD, Higgins DG. Fast, scalable generation of high-quality protein multiple sequence alignments using Clustal Omega. Mol Syst Biol. 2011;7:539.
29. Madeira F, Park YM, Lee J, Buso N, Gur T, Madhusoodanan N, Basutkar P, Tivey ARN, Potter SC, Finn RD, Lopez R. The EMBL-EBI search and sequence analysis tools APIs in 2019. Nucleic acids research. 2019;4:W636-W641.
30. Brown NP, Leroy C, Sander C. MView: a web-compatible database search ormultiple alignment viewer. Bioinformatics. 1998;14:380-1.

31. Kent WJ. BLAT–the BLAST-like alignment tool. Genome Res. 2002;**12:**656-664.
32. Labun K, Montague TG, Gagnon JA, Thyme SB, Valen E. CHOPCHOP v2: a web tool for the next generation of CRISPR genome engineering. Nucleic Acids Research. 2016;44:272-W276.
33. Lee CM, Cradick TJ, Fine EJ, Bao G. Nuclease target site selection for maximizing on-target activity and minimizing off-target effects in genome editing. Mol Ther NLM. 2016;24:475-487.
34. Farina JI, Molina OE, Figueroa LI. Formation and regeneration of protoplasts in *Sclerotium rolfsii* ATCC 201126. J Appl Microbiol. 2004;96:254-62.
35. Liu Z, Friesen TL. Polyethylene glycol (PEG)-mediated transformation in filamentous fungal pathogens. Methods Mol Biol. 2012;835:365-75.
36. Fariña JI, Siñeriz F, Molina OE, Perotti NI. Low-cost method for the preservation of *Sclerotium rolfsii* Proimi F-6656: Inoculum standardization and its use in scleroglucan production. Biotechnol Tech. 1996;10:705-708.
37. Survase SA, Saudagar PS, Singhal RS. Use of complex media for the production of scleroglucan by *Sclerotium rolfsii* MTCC 2156. Bioresour Technol. 2007;98:1509-1512.

Figures

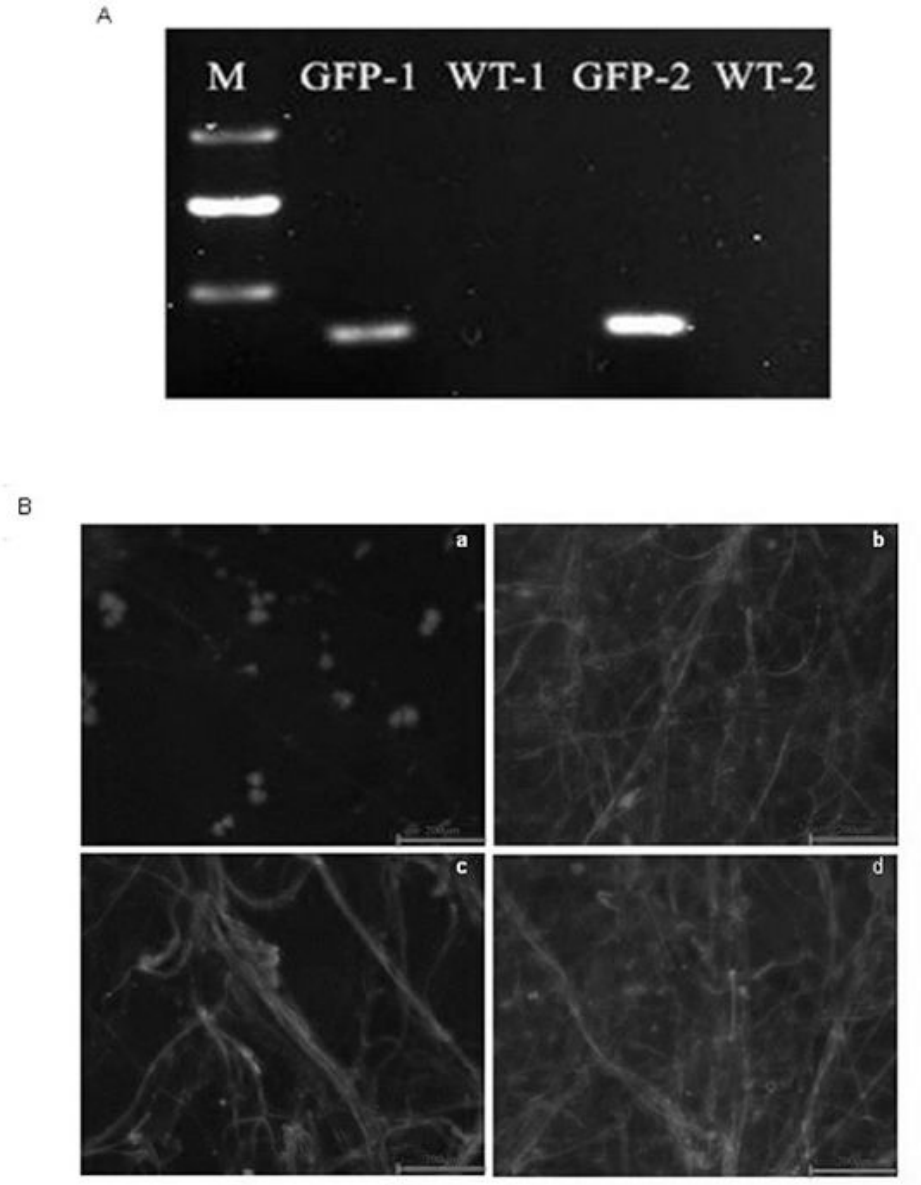

Figure 1

Identification of transformation for pDHt/sk-PE plasmid (A) GFP-1 and GFP-2 are transformants selected by hygromycin PDA top agar which could show 400bp band by using eGFP primers, however, the WT-1 and WT-2 could not. (B) (a) WT screened by microscope. (b c d) Three single colonies of transformants. Hyphae of WT could barely show green filamentous fluorescent, except the background signal from agar. In contrast, bright GFP fluorescent signal was shown in transformants

A

Mutations in AAT1-MT

GGCCCACGCCCACGGTTTGTCGTCCCGGTATG Wild type
GGC---CCCACGGTTTGgcgtcaTCGTCCCGGTATG -5 (-11, +6)
GG----GCCCACGCcatggTTTGTCGTCCCGGTATG -5 (-10, +5)
Ga-------CCCACGCccacgacatcgTCGTCCCGGTATG -6 (-18, +12)
GGCCCACGCCCACGacaTcGTCGTCCCGGTATG +1 (-3, +4)
GGCCCACGCCCACGacaTcGTCGTCCCGGTATG +1 (-3, +4)
GGCCCACGCCCACGGTTTGTCGTCCCGGTATG Wild type
GGCCCACGCCCACGGTTTGTCGTCCCGGTATG Wild type
GGCCCACGCCCACGGTTTGTCGTCCCGGTATG Wild type

B

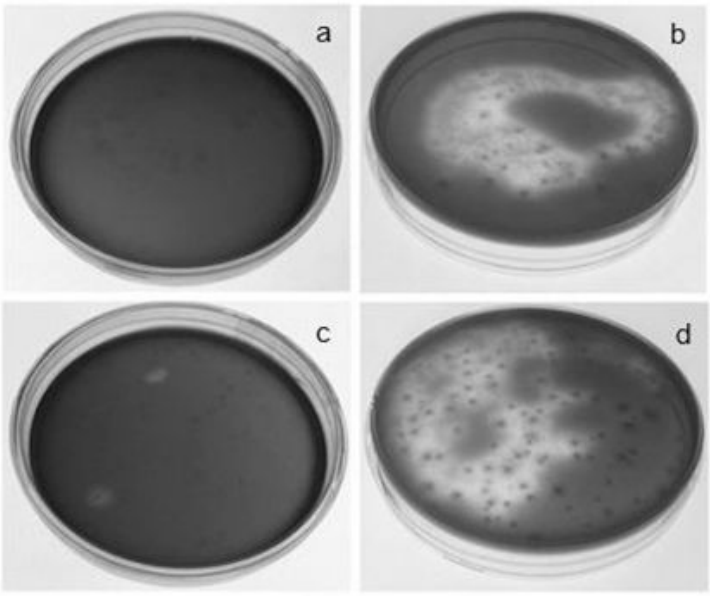

Figure 2

Selection and identification of mutants by hygromycin-BPDA medium and sequencing (A)Sequences of single colonies found after selection of our hyg-BPDA top agar. Deletions are marked by dashes. Insertions and the PAMs are marked in blue and purple, respectively. Numbers to the right of the sequences indicate the net loss or gain of bases for each sequence, with the number of bases inserted (+) or deleted (−) indicated in parentheses. (B) A fast method to select mutants compared with control

according to the medium color. Protoplasts of WT cultured in hygromycin-BPDA medium after 5 days (a) and 8 days (b), respectively. Protoplasts of S. rolfsii which has operated by PEG-mediated transformation of RNPs cultured in hygromycin-BPDA medium after 5 days (c) 8 days (d), respectively

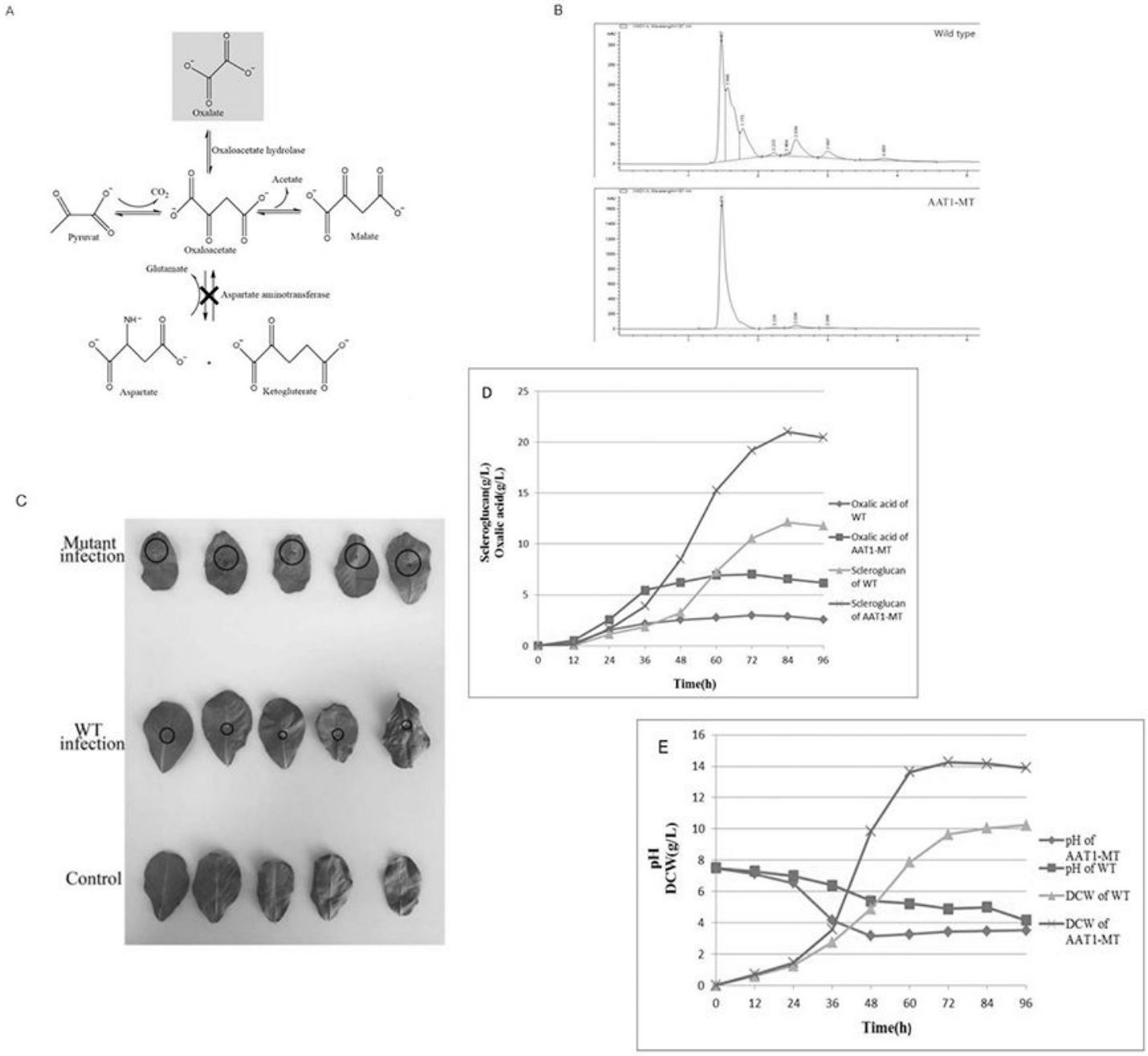

Figure 3

Comparison of WT and AAT1-MT with respect to oxalic acid production, bioassays, pH, DCW, and scleroglucan production (A) Metabolic pathway schematic of AAT1-MT. Inactivation of AAT1sequence is marked by cross, and the increased oxalic acid production was marked by red background. (B) Chromatogram of oxalic acid produced by WT and AAT1-MT in liquid medium, peaks were shown at retention time 1.4 min. Oxalic acid of mutants is distinctly increased compared with WT. (C) Bioassays of mutants in peanut leaves and controls strains. The lesion area caused by the erosion of acid metabolites, that is mainly oxalic acid, showed bright brown color, which is marked by black cycle. (D) The line chart

of scleroglucan and oxalic acid concentrations. Symbols: AAT1-MT scleroglucan concentration (×), WT scleroglucan concentration (▲), AAT1-MT oxalic acid concentration (■), WT oxalic acid concentration (□). (E) The line chart of pH and DCW concentrations. Symbols: AAT1-MT DCW concentration (×), WT DCW concentration (▲), pH of WT (■), pH of AAT1-MT(□). Each value represents the mean ± standard deviation of measurements from triplicate cultures.

Supplementary Files

This is a list of supplementary files associated with this preprint. Click to download.

- Supplementaryinformation.docx
- supplementarymaterial7.16.docx